

Speed Sensor less DTC of VSI fed Induction Motor with Simple Flux Regulation for Improving State Estimation at Low Speed

K. Farzand Ali¹, S.Sridhar²

¹ PG Scholar, Dept. Of Electrical & Electronics Engineering, JNTUACEA, Anantapuramu, A.P., India

² Asst. Professor, Dept. Of Electrical & Electronics Engineering, JNTUACEA, Anantapuramu, A.P., India

Abstract – In this paper constant switching frequency controller is used in order to replace 3-level hysteresis torque comparator without increasing the complexity of the control structure. The main objective of this paper is to improve speed and torque estimations of direct torque control of induction motor at low speed region with the improved flux regulation. It forms a simple structure of a look-up table based DTC drive by utilizing CSFC. With DTC-CSFC, constant switching frequency is maintained, and at the same time, poor stator flux regulation at low speed operation i.e. flux droop problem that normally occurs in DTC with the hysteresis controller (DTC-HC) at low speed is solved; and also the stator flux and torque estimations at low speed are also improved. By using an extended Kalman filter (EKF) based estimator the speed feedback for the closed loop speed control system is estimated, in the proposed system. Simulation work was carried out for the proposed work using MATLAB/SIMULINK software and results were presented for low speed operation.

Key Words: Constant switching frequency controller, direct torque control, extended Kalman filter, flux regulation, induction motor.

1. INTRODUCTION

Induction motor drives have been a mature technology for many years, but investigations into sensor less concepts are still taking place. The basic aim of sensor less control research is to achieve dynamic system performance equivalent to an encoded scheme without the disadvantages associated with using a speed encoder. Direct Torque Control was first introduced by Takahashi in 1986. It offers fast instantaneous torque and flux control with simple implementation. DTC controls the torque and speed of the motor, which is directly based on the electromagnetic state of the motor. The main advantages of DTC compared to FOC are less machine parameter dependence, simpler implementation and quicker dynamic torque response. And also it doesn't require the complex field orientation block, speed encoder, current regulator and PWM modulator. Even though DTC drives are inherently sensor less, the rotor speed information is still needed for the speed control, which is common in most industrial applications. However, rather than installing a mechanical speed

sensor, estimating the speed is more preferable as it reduces the drive cost, size, and maintenance requirements while increasing the system robustness and reliability. Processing requirements lower in DTC, whereas in FOC higher. No coordinate transforms are needed in DTC, all calculations are done in stationary coordinate frame.

DTC scheme has high efficiency & low losses. Switching losses are minimized because the transistors are switched only when it is needed to keep torque and flux within their hysteresis bands. In DTC, the step response has no overshoot. Typical control cycle time is 10-30 microseconds in DTC, where as in FOC it is 100-500 microseconds.

The main problems that are normally associated with DTC utilizing hysteresis torque controller (DTC-HC) are poor stator flux regulation at low speed operation, also referred as flux droop, high torque ripples and variable switching frequency. Problems of high torque ripples and variable switching frequency can be achieved by space vector modulation, known as the DTC-SVM. With DTC-SVM, voltage vector is generated within the sampling time, which is then synthesized using the space vector modulator, thus, hysteresis comparators are not needed for the flux and torque control. Nevertheless, the complexity of DTC structure and high computational effort increase significantly. Additionally, DTC-SVM cannot achieve stability at a zero speed operation. Flux droop problem, needs a separate treatment and cannot be directly solved with the implementation of DTC-SVM. With DTC-SVM, the torque and stator flux are indirectly controlled through the application of computed stator voltage space vectors. In order to solve this problem, it needs modifying the predefined lookup table of DTC-HC by adding more reverse voltage vectors to improve the flux regulation. However this leads to an increase in the size of the lookup table and require more precise stator flux position estimation.

In this paper, an alternative DTC variation with a constant switching frequency controller (DTC-CSFC) that retains the simple structure of DTC is presented. DTC-CSFC has been initially proposed, analyzed and proved for its capability in minimizing the torque ripple and operating at constant switching frequency. In this paper, the performance of DTC-CSFC near and at zero frequency is studied. With DTC-CSFC, flux regulation can be achieved

at low and zero frequency, which is a mandatory condition for any speed observer to work effectively. Also in this work, a speed estimator, which is based on an extended Kalman filter (EKF), is employed. The EKF based estimator has high convergence rate and good disturbance rejection, which can handle the model uncertainties and the effect of unmeasured disturbances. In general, EKF techniques currently employed for speed sensor less IM drives can be classified into two types: reduced order and full order estimators. The full order EKF type is more preferred and more widely used for the speed sensor less drive applications due to its better accuracy.

The control structure of the DTC of IM with Constant switching frequency controller is known for its simple structure and hence will be used in combination with the full order EKF. The CSFC is merely replacing the hysteresis torque controller without increasing the complexity of the control structure. The existence of stator currents and voltages due to the good flux regulation even at zero speed helps the EKF for improving the state estimation. Therefore, the EKF algorithm in its conventional form combined with DTC-CSFC, is preferable as it can provide improved performance at low and zero speed regions, with smaller sampling period, and hence achieving larger control bandwidth. With the improved with improved stator flux regulation, the performance of the estimator is good and acceptable

2. VOLTAGE SOURCE INVERTER (VSI)

A 3 phase two level voltage source inverter is used in direct torque control. The VSI synthesizes the voltage vectors commanded by the switching table. In DTC, this is quite simple since no pulse width modulation is employed; the output devices stay in the same state during the entire sample period.

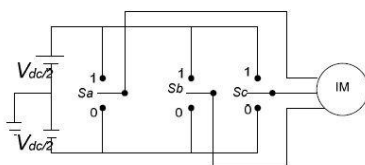


Fig. 1. Schematic diagram of VSI

A 3-phase VSI has eight possible configurations of six switches as shown in Fig .1. S_a , S_b , and S_c are the switching functions of each leg of the inverter. In each leg, the upper and lower switches are always complimentary to each other. S_a , S_b , or S_c equals to 1 indicates that the upper switch of the leg is ON while the value of 0 shows that the lower switch of the leg is ON. From the inverter switching modes, the line-to-neutral voltage v_a , v_b and v_c are determined. Eight different voltage vectors are specified according to the combination of the switching modes. The switching vectors associated with DTC are shown in Fig. 2. There are six active voltage vectors and

two zero voltage vectors at the origin. V_{dc} denotes the DC link voltage.

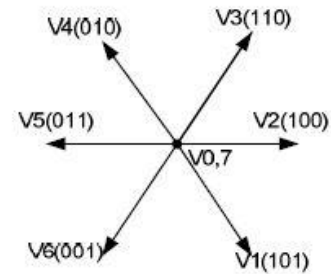


Fig. 2. Voltage vectors

$$V_s = \frac{2}{3} V_{dc} \left[S_a + e^{j\frac{2\pi}{3}} S_b + e^{j\frac{4\pi}{3}} S_c \right]$$

3. FLUX REGULATION OF BASIC DTC AT LOW SPEED

Direct torque control has received enormous attention in industrial motor drive applications. The main reason for its popularity is due to its simple structure, robustness against rotor parameter variations, and quick dynamic response.

The structure of basic DTC-HC, which was initially proposed, is shown in Fig. 3. Consist of voltage source inverter, Hysteresis flux controller, lookup table and flux and torque estimator. The output stator voltage is applied based on the selection of the switching states (S_a , S_b , S_c) obtained from a predetermined switching table, which is determined based the stator flux position and as to whether the torque and the stator flux need to be increased or decreased. The decouple control of torque and flux is accomplished by the three- and two-level hysteresis comparators of the torque and stator flux, respectively. The selection of suitable voltage vectors from the look-up table depends on the torque and stator flux demands.

The rate of change of stator flux vector is obtained from the stator voltage equation of IM expressed in stationary reference frame is given by (1).

$$\frac{d\psi_s}{dt} = V_s - i_s R_s \tag{1}$$

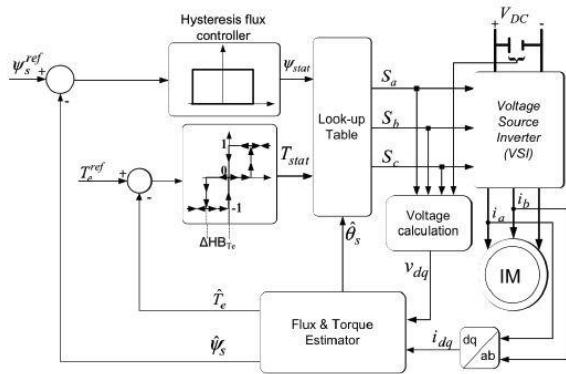


Fig. 3. Basic DTC-HC structure

Where ψ_s , v_s , and i_s , are the stator flux linkage, stator voltage and stator current space vectors respectively. R_s is the stator resistance.

For a short duration of time, (1) can be written as:

$$\Delta\Psi_{s1} = (V_s - i_s R_s) \Delta t \tag{2}$$

In Direct Torque Control of Induction Motor, when controlling the flux based on (2), it is a common practice to neglect the stator resistance drop when selecting voltage vectors from the look-up table. Therefore (2) can be approximated by (3):

$$\Delta\psi_s \approx v_s (\Delta t) \tag{3}$$

SELECTION OF VOLTAGE VECTOR

- 1) If flux need to be increased and torque need to be reduced during this condition Zero voltage vectors and reverse active voltage vectors will be selected.
- 2) If both flux and torque need to be increased during this condition forward voltage vectors will be selected.
- 3) If both flux and torque need to be reduced during this condition Zero voltage vectors and reverse active voltage vectors will be selected
- 4) If flux need to be reduced and torque need to be increased during this condition forward voltage vectors will be selected.

The selection of zero voltage vectors in order to reduce the torque is based on (3); it is assumed that the stator flux freezes ($\Delta\psi_s = 0$) when zero voltage vectors are selected. In actual, when the ohmic drop in (1) is considered, selection of a zero voltage vector resulted in a reduction in stator flux, as given by (4):

$$\Delta\psi_{s2} = -i_s R_s (\Delta t) \tag{4}$$

The change in stator flux in (4) is negligibly small, provided that the duration Δt is small and also when the motor current is small i.e. light load. The duration Δt

depends on how long it takes for the torque waveform to travel from upper to the lower band as shown in Fig. 4. Let the duration in which the torque travel from lower band to the upper band (positive torque slope) and from upper band to the lower band (negative torque slope) be Δt_1 and Δt_2 respectively.

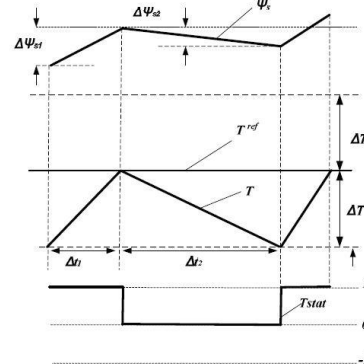


Fig. 4. Stator Flux and Torque Waveforms

Then from the figure it can be seen that in order for the flux to have a net positive increment, hence proper flux regulation,

$$\Delta\psi_{s1} > \Delta\psi_{s2} \tag{5}$$

Therefore we can write:

$$|(V_s - i_s R_s)| \Delta t_1 > |i_s R_s| \Delta t_2 \tag{6}$$

Since $\Delta T/\Delta t_1 = (\text{positive Tslope})$ and $\Delta T/\Delta t_2 = (\text{negative Tslope})$, we can write (5), which is the condition needed for flux regulation, as

$$\frac{\Delta t_1}{\Delta t_2} = \frac{\text{negative Tslope}}{\text{positive Tslope}} > \frac{|i_s R_s|}{|(V_s - i_s R_s)|} \tag{7}$$

Where the positive and negative torque slopes equations are given by equations (8.a) and (8.b),

$$(dT_e^+ / dt) = -T_e \{ (1/\sigma\tau_s) + (1/\sigma\tau_r) \} + \frac{3}{2} \frac{P}{\sigma} \frac{L_m}{\sigma L_s L_r} (V_s - j\omega_r \Psi_s) \cdot j \Psi_r \tag{8.a}$$

$$(dT_e^- / dt) = -T_e \{ (1/\sigma\tau_s) + (1/\sigma\tau_r) \} - \frac{3}{2} \frac{P}{\sigma} \frac{L_m}{\sigma L_s L_r} (j\omega_r \Psi_s) \cdot j \Psi_r \tag{8.b}$$

From equations (8.a) and (8.b), the dominant factor affecting the positive (dT_e^+ / dt) and negative (dT_e^- / dt) slopes is the rotor speed, ω_r . In general, the magnitude of the slopes will be influenced by the rotor speed.

VARIATION OF MAGNITUDE OF TORQUE SLOPES WITH SPEED

- 1) At low speed, positive slope will be high and negative slope will be low.
- 2) At medium speed, both the positive and negative slopes will be medium.
- 3) At high speed, positive slope will be low and negative slope will be high.

If $i_s R_s$ is neglected (i.e. $i_s R_s=0$), condition (7) is always true and hence stator flux can be regulated at all time. Since $|(V_s - i_s R_s)| > |i_s R_s|$ is true for most of the time, for high and medium speed regions, the ratio between the magnitudes of negative torque slope and positive torque slope equals unity or larger than unity, thus condition given by (7) is fulfilled. However at low speed region, the problem of stator flux regulation may occur. This happens when

$$\frac{\text{negativeTslope}}{\text{positiveTslope}} \leq \frac{|i_s R_s|}{|(V_s - i_s R_s)|} \tag{9}$$

We noted that the condition for proper flux regulation is determined by the ratio of negative and positive torque slopes. In order to avoid the condition in (9), one can either increase <negative T slope> or reduce <positive T slope>. The former can be accomplished by selecting reverse voltage vectors when the torque needs to be reduced, whereas the latter can be fulfilled by selecting voltage vectors with less tangential component whenever the torque needs to be increased. Using the reverse voltage vectors or more radial voltage vectors will unnecessarily increase the switching frequency at low speed and can also increase the torque ripple. And also it requires a modification of lookup table at different low and high speeds.

4. IMPROVED FLUX REGULATION USING DTC-CSFC AT LOW SPEED

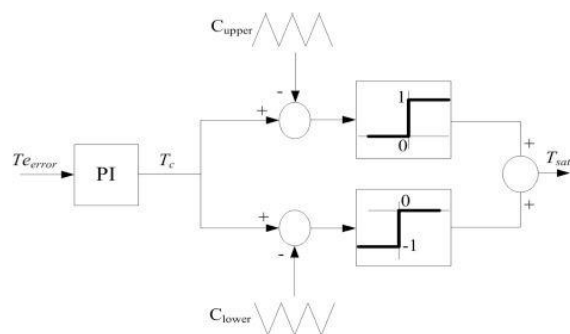


Fig. 5. Constant Switching Frequency Controller

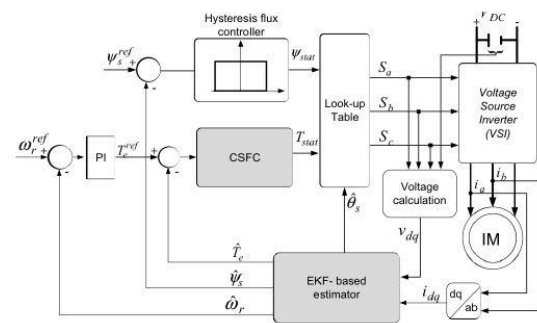


Fig. 6. The proposed EKF- based DTC-CSFC

Torque Hysteresis controller used in existing system can be replaced by Constant Switching Frequency Controller (CSFC). The DTC of IM incorporating the CSFC is shown in Fig. 5. The DTC-CSFC system can have voltage source inverter(VSI), look-up table,hysteresis flux controller, constant switching frequency controller, PI controller and EKF based estimator. DTC-CSFC consists of two comparators that compare two constant frequency triangular waveforms (C_{upper} and C_{lower}) with a compensated torque error (T_c). The controller output (T_{sat}) produces similar output pattern as the conventional three level hysteresis comparator but with constant switching frequency as given by:

$$T_{sat} = \begin{cases} 1, & T_c \geq C_{upper} \\ 0, & C_{lower} < T_c < C_{upper} \\ -1, & T_c \leq C_{lower} \end{cases} \tag{10}$$

The flux regulation in DTC-CSFC at low speed is improved due to the selection of the reverse voltage vectors by the CSFC when regulating the torque; reverse voltage vectors produce steeper negative torque slope compared to zero voltage vectors therefore fulfilling (7).

In DTC-HC, selection of reverse voltage vectors requires modification to the lookup table. But in DTC-CSFC it doesn't required. At low speed and light load, reverse voltage vectors will be selected naturally whenever T_c crosses the lower triangular waveform. Simulation of closed-loop speed control of DTC-CSFC is conducted to an IM with parameters given in Fig. 7, Fig. 8 and Fig.9

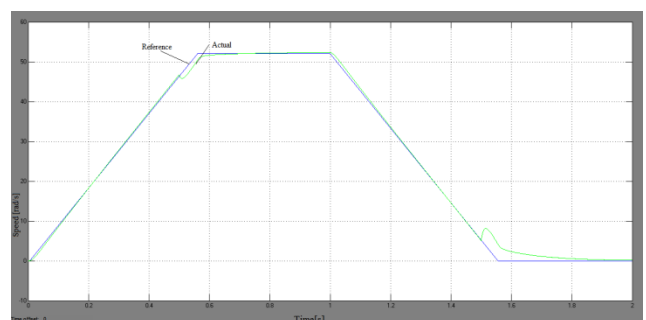


Fig.7. Speed [rad/s]

In Fig. 7, a step change in speed from 0 to 52 rad/s is applied at t=0 sec. At t= 1.6 sec the speed reference is stepped down to 5 rad/s

$$f_i(x_i(t), u(t)) = A_i(x_i(t), x_i(t)) + B u(t) \tag{12}$$

$$Y(t) = H_i(x_i(t), x_i(t)) + B u(t) + v_i(t) \tag{13}$$

where $i = 1, 2$, extended state vector x_i is the estimated states of the IM, f_i is the nonlinear function of the states and inputs, A_i is the system matrix, u is the control-input vector, B is the input matrix, w_i is the process noise, H is the measurement matrix, and v_i is the measurement noise and Y is the output system matrix. The noisy signals w_i and v_i are regarded as zero mean, white noise, and being totally uncorrelated with each other. The detailed representation of (11) and (13) are given in the following state space form:

$$\dot{x} = Ax + Bu + w(t) \tag{14}$$

Where,

$$\dot{x} = [isd \quad isq \quad \Psi_{rd} \quad \Psi_{rq} \quad \omega r]^T$$

$$x = [isd \quad isq \quad \Psi_{rd} \quad \Psi_{rq} \quad \omega r]^T$$

$$A = \begin{bmatrix} \frac{k1}{L\sigma} & 0 & \frac{Lm}{L\sigma Lr Tr} & \frac{\omega r Lm}{L\sigma Lr} & 0 \\ 0 & -\frac{k1}{L\sigma} & -\frac{\omega r Lm}{L\sigma Lr} & \frac{Lm}{L\sigma Lr Tr} & 0 \\ \frac{Lm}{Tr} & 0 & -\frac{1}{Tr} & -\omega r & 0 \\ 0 & \frac{Lm}{Tr} & \omega r & -\frac{1}{Tr} & 0 \\ 0 & 0 & 0 & 0 & 0 \end{bmatrix}$$

$$B = \begin{bmatrix} \frac{1}{L\sigma} & 0 \\ 0 & \frac{1}{L\sigma} \\ 0 & 0 \\ 0 & 0 \\ 0 & 0 \end{bmatrix}$$

$$u = \begin{bmatrix} vsd \\ vsq \end{bmatrix}$$

Here,

$$T_r = \frac{L_r}{R_r};$$

$$K1 = R_s + (L_m^2 / L_r T_r);$$

$$L_\sigma = L_s - (L_m^2 / L_r);$$

$$Y = Hx + v(t) \tag{15}$$

Where, $Y = \begin{bmatrix} isd \\ isq \end{bmatrix}$, $H = \begin{bmatrix} 1 & 0 & 0 & 0 & 0 \\ 0 & 1 & 0 & 0 & 0 \end{bmatrix}$

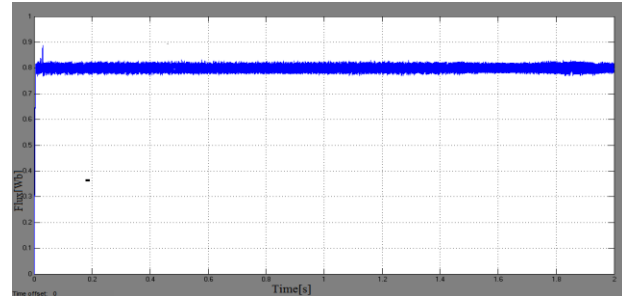


Fig. 8. Flux [Wb]

In Fig. 8, At low speed, i.e., less than 5 rad/sec stator flux regulation can be maintained i.e., it is maintained to be good.

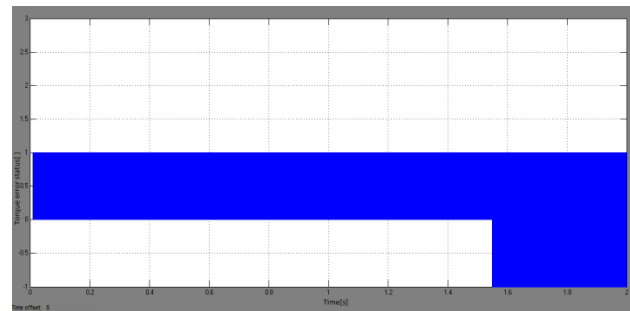


Fig. 9. T_{sat} Torque error status

In Fig. 9, The waveform of T_{sat} indicated that reverse voltage vectors are selected for DTC-CSFC, which is the reason behind the proper flux regulation. Selection of the reverse voltage vectors increases the overall magnitude of the negative slope, and also fulfils the requirement for flux regulation.

5. EXTENDED KALMAN FILTER ALGORITHM

The Kalman filter (KF) is a predictor and correcting type estimator used for stochastic estimation. It is an optimal estimator in the sense of minimising the estimated error covariance. Due to the non-linearity of our IM system and the need for its linearization, extended Kalman filter (EKF) is applied in this study to simultaneously estimate stator current, rotor flux, and motor speed for speed sensor less control of IM. Nevertheless, the correct estimation of EKF states is much reliable on the accurate choice of the filter matrices for a wide speed range. The extended model to be used in the EKF algorithm can be expressed in the following general form (as referred to the stator stationary frame):

$$\dot{x}_i(t) = f_i(x_i(t), u(t)) + w_i(t) \tag{11}$$

where i_{sd} and i_{sq} are the d and q components of stator current, Ψ_{rd} and Ψ_{rq} are d-q rotor flux, ω_r is the rotor electric angular speed in rad/s, v_{sd} and v_{sq} are the stator voltage components, L_s , L_r and L_m are the stator, rotor and mutual inductances respectively, σ is the total leakage factor, specified by $\frac{1-L_m^2}{L_s L_r}$, R_s is the stator resistance, and R_r is the rotor resistance.

The EKF algorithm used in the stationary reference frame of IM model is derived using the extended model in (14) and (15). Due to the non-linearity of IM states, the EKF scheme attempts to solve this issue by using a linearized approximation, where the linearization is performed about the recent state estimate. This process involves the discretization of (14) and (15) is as follows:

$$\dot{x}_i(k) = f_i(x_i(k), u(k)) + w_i(k) \tag{16}$$

$$f_i(x_i(k), u(k)) = A_i(x_i(k), x_i(k)) + B u(k) \tag{17}$$

$$Y(k) = H_i(x_i(k), x_i(k)) + B u(k) + v_i(k) \tag{18}$$

The linearization of (7) is performed around the current estimated state vector \hat{x}_i given as follows:

$$F_i(k) = \left. \frac{\partial f_i(x_i(k), u(k))}{\partial x_i(k)} \right|_{\hat{x}_i(k)} \tag{19}$$

Finally, the resulting EKF algorithm can be given with the following recursive equations:

$$P(k) = F(k) P(k) F(k)^{-1} + Q \tag{20}$$

$$K(k+1) = H^T P(k) (H P(k+1) H^T + R)^{-1} \tag{21}$$

$$\hat{x}(k+1) = \hat{f}(x(k), u(k)) + K(k) \cdot (Y(k) - H \hat{x}(k)) \tag{22}$$

$$P(k+1) = (1 - k(k+1)H) P(k) \tag{23}$$

In (10)-(13) Q is the covariance matrix of the system noise, namely, model error, R is the covariance matrix of the output noise, namely, measurement noise, and P are the covariance matrix of state estimation error. The algorithm involves two main stages: prediction and filtering. In the prediction stage, the next predicted states $\hat{f}(\cdot)$ and predicted state-error covariance matrices, $\hat{P}(\cdot)$ are processed, while in the filtering stage, the next estimated states $\hat{x}(k+1)$ obtained as the sum of the next predicted states and the correction term [second term in (12)], are calculated.

The voltage d and q components in (4) can be obtained from the switching pattern of the 3-phase voltage source inverter as follows.

$$V_{sd} = \frac{1}{3} V_{DC} (2S_a - S_b - S_c) \tag{24}$$

$$V_{sq} = \frac{1}{\sqrt{3}} V_{DC} (S_b - S_c) \tag{25}$$

Where V_{DC} is the DC supply voltage and S_a , S_b , and S_c are selected signals that represent phases a , b , and c respectively obtained from the lookup table. From the estimated rotor speed and rotor flux linkage values using EKF filter, the stator flux can be obtained using the following.

$$\Psi_{sd} = \frac{L_m}{L_r} \Psi_{rd} + L_\sigma i_{sd} \tag{26}$$

$$\Psi_{sq} = \frac{L_m}{L_r} \Psi_{rq} + L_\sigma i_{sq} \tag{27}$$

The electromagnetic torque based on EKF is calculated based on the selected state variables which are the stator current and rotor flux:

$$T_e = \frac{3}{2} \frac{P}{2} \frac{L_m}{L_r} (i_{sq} \Psi_{rd} - i_{sd} \Psi_{rq}) \tag{28}$$

6. CONCLUSIONS

In this paper, hysteresis torque controller is replaced by using constant switching frequency controller in order to improve the flux regulation of a lookup table based DTC. The state estimations at very low and zero speed operations are also improved with the improved flux regulation. Even though EKF based estimator has been used to estimate the stator and rotor fluxes and the speed, the simple structure of DTC-CSFC has made it possible for the sampling time of the system to be reduced. A closed-loop speed control is constructed by using the estimated speed as the feedback in order to test the performance of DTC-CSFC.

APPENDIX

INDUCTION MACHINE PARAMETERS AND DTC-CSFC VALUES

Induction Machine		Hysteresis flux controller and CSFC	
Rated power	1.5 kW	Flux hysteresis band	0.025 Wb
Rated current	3.67A	Proportional gain	6.6653
Stator resistance	3	Ohm Integral gain	1221.83
Rotor resistance	4.1	Ohm Carrier frequency	2272 Hz
Stator self inductance	0.3419 H	Peak to peak of carrier freq.	100
Rotor self inductance			

0.3513 H	
Mutual inductance 0.324 H	
Number of pole pair 2	
Rated stator flux 0.954 Wb	
Torque rated 9 Nm	

Power Electronics, Drives and Energy Systems Conf., 2012, pp. 1-6.

- [11] L. Harnefors and M. Hinkkanen, "Stabilization Methods for Sensorless Induction Motor Drives—A Survey," *IEEE JOURNAL OF EMERGING AND SELECTED TOPICS IN POWER ELECTRONICS*, vol. 2, pp. 132-142, 2014.
- [12] D. Stojić, M. Milinković, S. Veinović, and I. Klasnić, "Improved Stator Flux Estimator for Speed Sensorless Induction Motor Drives," *IEEE Trans. Power Electronics*, vol. 30, pp. 2363-2371, 2015.

REFERENCES

- [1] I. Takahashi and T. Noguchi, "A New Quick-Response and High-Efficiency Control Strategy of an Induction Motor," *IEEE Trans. Ind. App.*, vol. IA-22, pp. 820-827, 1986.
- [2] A. B. Jidin, N. R. B. N. Idris, A. B. M. Yatim, M. E. Elbuluk, and T. Sutikno, "A Wide-Speed High Torque Capability Utilizing Overmodulation Strategy in DTC of Induction Machines With Constant Switching Frequency Controller," *Power Electronics, IEEE Transactions on*, vol. 27, pp. 2566-2575, 2012.
- [3] I. M. Alsofyani and N. R. N. Idris, "A review on sensorless techniques for sustainable reliability and efficient variable frequency drives of induction motors," *J. Renewable and Sustainable Energy Reviews*, vol. 24, pp. 111-121, 2013.
- [4] J. W. Finch and D. Giaouris, "Controlled AC Electrical Drives," *IEEE Trans. Ind. Electron.*, vol. 55, pp. 481-491, 2008.
- [5] G. S. Buja and M. P. Kazmierkowski, "Direct torque control of PWM inverter-fed AC motors - a survey," *IEEE Transactions on Industrial Electronics*, vol. 51, pp. 744-757, 2004.
- [6] Z. Yongchang and Z. Jianguo, "A Novel Duty Cycle Control Strategy to Reduce Both Torque and Flux Ripples for DTC of Permanent Magnet Synchronous Motor Drives With Switching Frequency Reduction," *IEEE Trans. Power Electronics*, vol. 26, pp. 3055-3067, 2011.
- [7] N. R. N. Idris and A. H. M. Yatim, "Direct torque control of induction machines with constant switching frequency and reduced torque ripple," *IEEE Trans. Ind. Electron.*, vol. 51, pp. 758-767, 2004.
- [8] A. Jidin, N. R. N. Idris, A. H. M. Yatim, A. Z. Jidin, and T. Sutikno, "Torque ripple minimization in DTC induction motor drive using constant frequency torque controller," in *Proc. IEEE Electrical Machines and Systems Conf.*, 2010, pp. 919-924.
- [9] C. Patel, R. P. P. A. Day, A. Dey, R. Ramchand, K. Gopakumar, and M. P. Kazmierkowski, "Fast Direct Torque Control of an Open-End Induction Motor Drive Using 12-Sided Polygonal Voltage Space Vectors," *IEEE Trans. Power Electronics*, vol. 27, pp. 400-410, 2012.
- [10] C. M. Sanila, "Direct Torque Control of induction motor with constant switching frequency," in *Proc. IEEE*